

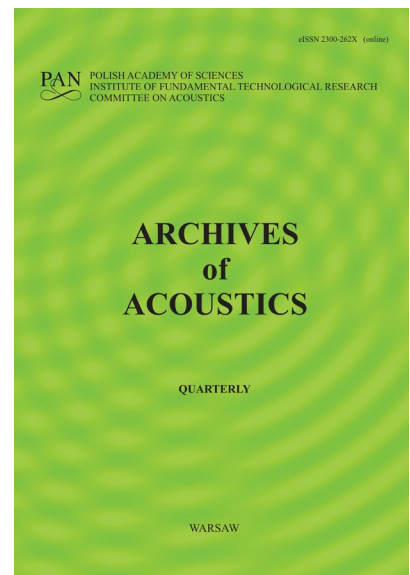
JOURNAL PRE-PROOF

This is an early version of the article, published prior to copyediting, typesetting, and editorial correction. The manuscript has been accepted for publication and is now available online to ensure early dissemination, author visibility, and citation tracking prior to the formal issue publication.

It has not undergone final language verification, formatting, or technical editing by the journal's editorial team. Content is subject to change in the final Version of Record.

To differentiate this version, it is marked as "PRE-PROOF PUBLICATION" and should be cited with the provided DOI. A visible watermark on each page indicates its preliminary status.

The final version will appear in a regular issue of *Archives of Acoustics*, with final metadata, layout, and pagination.



Title: Laboratory Evaluation of Underwater Acoustic Attenuation Provided by Air Bubble Curtains

Author(s): Alfio Yori, Jose Luis Barros, Rodrigo Torres, Felipe Figueroa

DOI: <https://doi.org/10.24423/archacoust.2026.4254>

Journal: *Archives of Acoustics*

ISSN: 0137-5075, e-ISSN: 2300-262X

Publication status: In press

Received: 2025-06-03

Revised: 2025-12-26

Accepted: 2026-01-01

Published pre-proof: 2026-01-16

Please cite this article as:

Yori A., Barros J.L., Torres R., Figueroa F. (2026), Laboratory Evaluation of Underwater Acoustic Attenuation Provided by Air Bubble Curtains, *Archives of Acoustics*, <https://doi.org/10.24423/archacoust.2026.4254>

Copyright © 2026 The Author(s).

This work is licensed under the Creative Commons Attribution 4.0 International CC BY 4.0.

Laboratory Evaluation of Underwater Acoustic Attenuation Provided by Air Bubble Curtains

Alfio YORI^{1,*}, José Luis BARROS¹, Rodrigo TORRES¹, Felipe FIGUEROA¹

¹ Instituto de Acústica, Universidad Austral de Chile, Valdivia, Chile

* Corresponding author email: ayori@uach.cl

Summary

Air bubble curtains are widely used in Chilean salmon farming to protect fish from water pollutants. Due to new requirements from the Chilean Environmental Assessment Service, their use for underwater noise mitigation has become very important. This study aimed to evaluate the acoustic attenuation provided by a type of curtain widely used in salmon farming and seawater desalination under laboratory conditions, obtaining results independent of the conditions encountered in field work. This allowed for comparative measurements of different bubble curtain configurations. This study presents the results of an acoustic evaluation of underwater sound attenuation provided by different bubble curtain configurations, conducted in the test channel of the Engineering Department at the Universidad Austral de Chile. The parameter evaluated was insertion loss IL . It was found that the bubble curtains evaluated provided a broadband insertion loss between 11 dB and 12 dB in the simplest configuration and an Insertion Loss IL per third-octave band equal to or greater than 10 dB. A 10 dB attenuation in the source level represents a significant reduction in the area of acoustic impact, reducing the physiological damage distances for the marine mammal species considered by at least 78.4%.

Keywords: Air-bubble curtain, underwater sound attenuation, reduction of physiological risk, underwater noise control.

1 Introduction

Currently, in Chile, bubble curtains are widely used in salmon farming centers to protect salmon from algae blooms or waterborne solid and liquid contaminants. Another use of these bubble curtains, which has been steadily increasing in our country, is in the water intake pipes of desalination plants to prevent the suction of organic matter. Due to new requirements of the Chilean Environmental Assessment Service (SEA, 2022) (SEA, 2022), regarding the impact of underwater noise, a new need arises for the use of bubble curtains to mitigate anthropogenic underwater noise.

The efficacy of bubble curtains in regulating the dispersal of both solid and oil contaminants can be demonstrated visually. However, validating their effectiveness in sound attenuation poses a greater challenge. Despite the ambiguity surrounding the quantification of the effectiveness of bubble curtains in reducing underwater noise, they are generally recommended as a possible strategy for mitigating the acoustic impact on marine organisms. One of the reasons why information about the acoustic effectiveness of these curtains presents high variability is the

36 lack of attenuation measurements under controlled conditions (Rustemeier *et al.*, 2012; Beelen
 37 *et al.*, 2025), contrasted with the high number of field measurements (CALTRANS, 2020;
 38 Würsig *et al.*, 2000; Dähne *et al.*, 2017; Lucke *et al.*, 2011) and computerized models studies
 39 (Novarini *et al.*, 2017; Hall, 1989; Götsche *et al.*, 2013; Chao *et al.*, 2021; Tsouvalas, 2020).

40 Air bubble curtains can be used as underwater acoustic barriers to control underwater noise
 41 sources and reduce acoustic impacts in the marine environment. Air bubble curtains are one of
 42 the few mitigation measures available for controlling anthropogenic underwater noise. (Stri-
 43 etman *et al.*, 2018; Koschinski, Ludemann, 2013; OSPAR, 2014; Bellmann, 2014; JNCC, 2010;
 44 Werner, 2010; Lucke, Siemensma, 2013). Currently, the Chilean Environmental Assessment
 45 Agency (SEA, 2022) requires that projects with potential underwater acoustic impacts include
 46 mitigation measures, with air bubble curtains being a possible solution.

47 Due to this lack of information or clarity about sound attenuation provided by the air-bubble
 48 curtains, the main objective of this work is to assess, under controlled laboratory conditions,
 49 the acoustic attenuation provided by a type of curtain widely used by both the salmon industry
 50 and the industries of sea-water desalination as well; seeking to achieve results independent
 51 from those variable conditions so commonly present in field measurements. Thus, attenuation
 52 results obtained from different curtains configurations may be compared.

53 This work shows the results of the acoustic assessment of underwater sound attenuation
 54 given by different configurations of air-bubble curtains, which was carried out in the test-
 55 channel belonging to the Engineering Faculty from Universidad Austral de Chile. The assessed
 56 parameter was Insertion Loss *IL*, estimated from the sound pressure level generated by a sound
 57 source over a hydrophone, with and without the presence of the evaluated attenuating element
 58 (Fahy, 2001).

59 2 Objectives

- 60 • To measure, under controlled conditions, underwater sound attenuation provided by air-
 61 bubble curtains presently used in the control of solid and liquid particles in salmon farming
 62 and water desalination plants.
- 63 • To evaluate the reduction in the acoustic impact area of a project involving underwater
 64 noise and marine mammals when air bubble curtains are used as a mitigation measure.

65 3 Theoretical Framework

66 3.1 Underwater Sound Generalities

67 In air acoustics, the standard reference pressure $p_0 = 20[\mu\text{Pa}]$ corresponds to the threshold of
 68 human hearing. In contrast, underwater acoustics uses a different reference pressure (Robinson
 69 *et al.*, 2014; Möser, Barros, 2004) equal to $p_0 = 1[\mu\text{Pa}]$. It is important to note that, due to
 70 significant differences in the acoustic impedance of air and water, sound pressure levels between
 71 these two media cannot be directly compared. For example, even in extremely quiet underwater
 72 environments, the broadband background noise level is generally around 90 dB re.1 $[\mu\text{Pa}]$. Under
 73 high wind conditions, this value may reach approximately 120 dB re.1 $[\mu\text{Pa}]$ (Richardson *et al.*,
 74 1995; Urick, 2010).

3.2 Sound and Marine Mammals

Anthropogenic underwater noise in the oceans can negatively affect mammals and invertebrates. In the oceans, sound propagates efficiently, just as light does in air (Richardson *et al.*, 1995). Marine mammals have evolved, taking advantage of the phenomenon of low sound attenuation using their hearing for most tasks, whereas land mammals use their eyesight. Thus, marine mammals use hearing for critical tasks such as navigation, communication, prey hunting, predator detection, and spatial localization in the dark ocean (Richardson *et al.*, 1995; Urick, 2010; DAHG, 2014). Marine mammals can be mainly divided into (DPTI, 2012):

- Mysticetes or baleen whales, where this group includes large whales such as right whales, sei whales, humpback whales and blue whales. These species produce sounds mainly under 1000 Hz; with notable exceptions such as the humpback whale, which emits frequencies exceeding 1000 Hz, and the blue whale, which emits frequencies as low as 10-15 Hz.
- Odontocetes or toothed whales, in which dolphins, killer whales, sperm whales and porpoises are included. This type of cetacean communicates using frequencies under 20 kHz and use high-frequency echolocation to perceive their surroundings, using frequencies over 20 kHz.
- Pinnipeds, which include sea lions and sea elephants, communicate using frequencies ranging from 1 to 4 kHz.

3.3 Physiological and Behavioral Impact Due to Underwater Noise

The effects of underwater noise of anthropogenic origin over marine mammals may be divided into five categories, which depend on the distance between the receiver and the sound source (DAHG, 2014; DPTI, 2012; MacKenzie, 2015).

- Physiological stress response.
- Behavioral response.
- Masking.
- Temporary threshold shift TTS.
- Permanent threshold shift PTS or physical damage

The frequency ranges through which these five groups of animals communicate are not well defined, and the levels of sound vary significantly between species. The range over which sounds can be detected depends largely on background noise levels and the animal's hearing threshold. Figure 1 shows a comparative graph of the average hearing thresholds of different mammal groups.

Masking is an effect whereby noise masks essential auditory signals for animals, such as communication, obstacles or predator detection.

Changes in behaviour are observed across a wide range of sound levels but are difficult to evaluate objectively, since an animal's reaction to a noise depends on factors such as the type of sound, exposure time, and the season.

A TTS indicates temporary deafness, whereas a PTS implies a irreversible hearing loss. (DAHG, 2014; DPTI, 2012; MacKenzie, 2015).

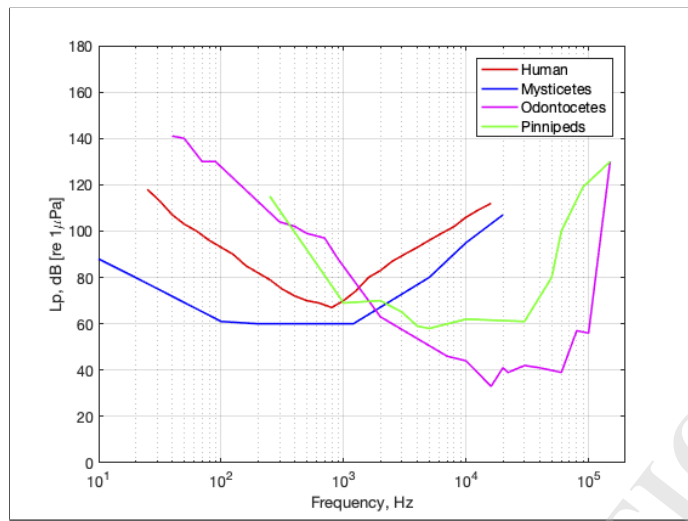


Figure 1: The average hearing thresholds of different groups of marine mammals, and humans when underwater (Parvin, Nedwell, 1995; Nedwell *et al.*, 2004)

114 It is important to note that not all high-level sounds will be harmful for all species. The
 115 auditory perception of a sound is considered harmful only if its frequencies fall within the
 116 audible range of the species concerned. Secondly, the level must exceed the initial level at
 117 which the species begins to perceive sound, around 50 dB (Richardson *et al.*, 1995; Nedwell
 118 *et al.*, 2007).

119 Figure 2 shows a comparison of the frequency spectrum of pile driving noise at a distance
 120 of 25 m (Yori, 2018) with the hearing thresholds of different species (Nedwell *et al.*, 2004).
 121 Frequency spectrum measured during the driving of piles 0.61 m in diameter, with a D62 diesel
 122 hammer and 40 blows per minute.

123 **3.3.1 Criteria for the Assessment of Underwater Noise Impact NOAA NMFS
 124 2018/2024**

125 The National Marine Fishing Service NMFS of United States, belonging to the National Office
 126 of Ocean and Atmospheric Administration, NOAA, organized, interpreted and synthesized
 127 available scientific information regarding the impact of underwater noise over marine mammals,
 128 to, afterwards, define maximum thresholds to avoid the occurrence of a temporal hearing shifts
 129 TTS or an auditory injury AUD INJ, where AUD INJ includes, but is not limited to PTS.
 130 Marine mammals are grouped into seven groups as shown in Table 1.

131 The noise levels used by NMFS criteria to assess the impact of underwater noise on marine
 132 mammals are summarized in Table 2 (NOAA, 2024). Levels presented in Table 2 are cumulative
 133 and weighted levels, therefore the frequency spectrum amplitudes of the assessed noise must be
 134 weighted by the auditory weighting functions corresponding to each group in Table 1. These
 135 auditory weighting functions curves represent the hearing characteristics of the species classified
 136 in each one of these groups.

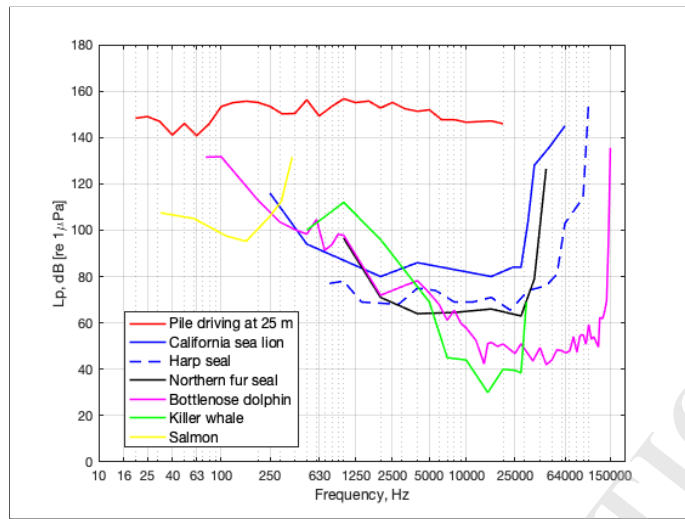


Figure 2: Spectrum of a pile driving noise in 1/3 octave bands, in contrast with the audiograms of different species (Yori, 2018; Nedwell *et al.*, 2004)

Table 1: Hearing groups and ranges according to criterion NMFS 2024 (NOAA, 2024).

Hearing group	Hearing range
Low-frequency (LF) cetaceans (baleen whales)	7 Hz a 36 kHz
High-frequency (HF) cetaceans (dolphins, toothed whales, beaked whales, bottlenose whales)	150 Hz a 160 kHz
Very High-frequency (VHF) cetaceans (true porpoises, <i>Kogia</i> , river dolphins, cephalorhynchid, <i>Lagenorhynchus cruciger</i> , <i>L. australis</i>)	200 Hz a 165 kHz
Phocid pinnipeds (PW) (underwater) (true seals)	40 Hz a 90 kHz
Otariid pinnipeds (OW) (underwater) (sea lions and fur seals)	60 Hz a 39 kHz
Phocid pinnipeds (PA) (air) (true seals)	42 Hz a 52 kHz
Otariid pinnipeds (OA) (air) (sea lions and fur seals)	90 Hz a 40 kHz

Table 2: Thresholds for assessing the acoustic impact of underwater noise. Auditory injury INJ and temporal threshold shift TTS according to NMFS 2024 criterion (NOAA, 2024). dB re.1[μ Pa² · s]

Group	Non-impulsive noise		Impulsive noise	
	Threshold TTS SEL_{cum24h} , dB	Threshold AUD INJ SEL_{cum24h} , dB	Threshold TTS SEL_{cum24h} , dB	Threshold AUD INJ SEL_{cum24h} , dB
LF	177	197	168	183
HF	181	201	178	193
VHF	161	181	144	159
OW	179	199	170	185
PW	175	195	168	183

137 4 Materials and Methods

138 4.1 Measurement System

139 The system employed for the measurement of underwater acoustic attenuation, provided by
 140 the evaluated air bubble curtain, was as follows:

- 141 • Loudspeaker Lubell Labs, model LL916H [Frequency Response: 200 Hz - 23 kHz (± 15 dB) and 500 Hz - 21 kHz (± 10 dB)].
- 142 • Amplifier Peavey, model 2600, 75 watt RMS.
- 143 • Sound level meter NTI, type 1, model XL2
- 144 • Hydrophone Cetacean Research Technology, model C55 [Frequency Response: 15 Hz - 44 kHz (± 3 dB) and 8 Hz - 100 kHz (± 12 dB)].
- 145 • Eight-track recorder Tascam, model DR680.
- 146 • Power source Cetacean Research Technology model 736.
- 147 • White noise source.

150 It is important to note that the speaker used is capable of emitting sound below 200 Hz.
 151 According to the sound pressure level plot provided by the manufacturer, the speaker is capable
 152 of producing a sound pressure level of 130 dB re.1[$\mu\text{Pa}\cdot\text{m}$] below 40 Hz.

153 4.2 Hydrodynamic Testing Channel and Bubble Curtain Installation

155 The measurement was carried out in the hydrodynamic testing channel of the Engineering
 156 Faculty at Universidad Austral de Chile (see Figure 3). The channel is 50 m in length, 3 m
 157 in width, and 1.7 m in depth, and is constructed from steel. In principle, the water depth is
 158 capable of providing a work range above 200 Hz, given that lower frequencies are not propagated
 159 along the channel (Richardson *et al.*, 1995; Urick, 2010). However, near the source, there is
 160 propagation below this cut-off frequency, but its amplitude decays after a few wavelengths.
 161 (Möser, Barros, 2004).

162 As demonstrated in Figures 4 and 5, the distance between the sound source and the hydrophone is 20 m. The evaluation involved four configurations of the curtain, with each line
 163 comprising two diffusers and hoses. The lines are designated Line 1, Line 2, Line 3, and Line 4,
 164 with their respective locations being 5 m, 7 m, 10 m, and 15 m from the sound source. Figure
 165 6 shows one of these lines, where each hose has a 3/4-inch diameter and is supplied with an
 166 air flow rate of 27 l/min. The hoses have membranes producing microbubbles with diameters
 167 between 1 mm and 5 mm.

168 Each measurement was repeated four times, with the hydrophone positioned in four different
 169 locations, as illustrated in Figure 7. The objective of these four positions was to minimize the
 170 effect of finding the hydrophones at a position coinciding with a sound field diminishing at the
 171 point due to interference. This phenomenon was also reported in previous studies (Beelen *et*
 172 *al.*, 2025), so the goal here was to improve the ratio of sound signal to background noise. To get
 173 an average value reflecting both time and space, the results from these four different positions
 174 were combined by calculating their mean energy.



Figure 3: Hydrodynamic testing channel.

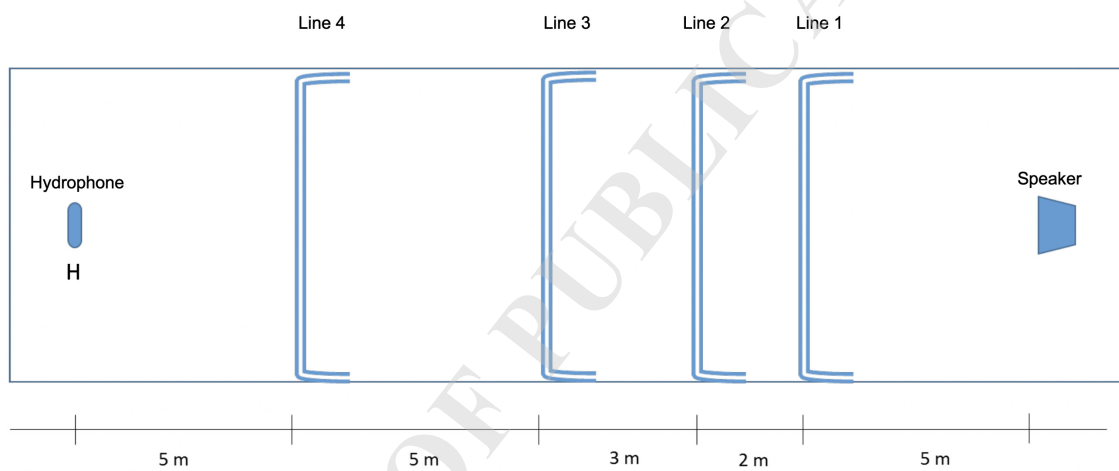


Figure 4: Spatial arrangement of the four lines assessed in the study.

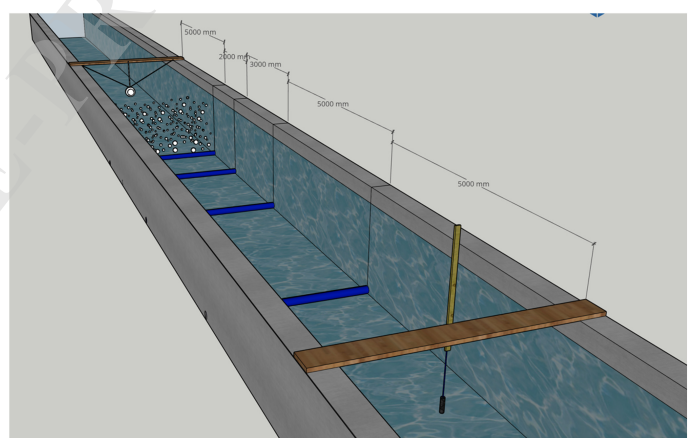


Figure 5: Operational sequence of Line 1 producing its bubble curtain.

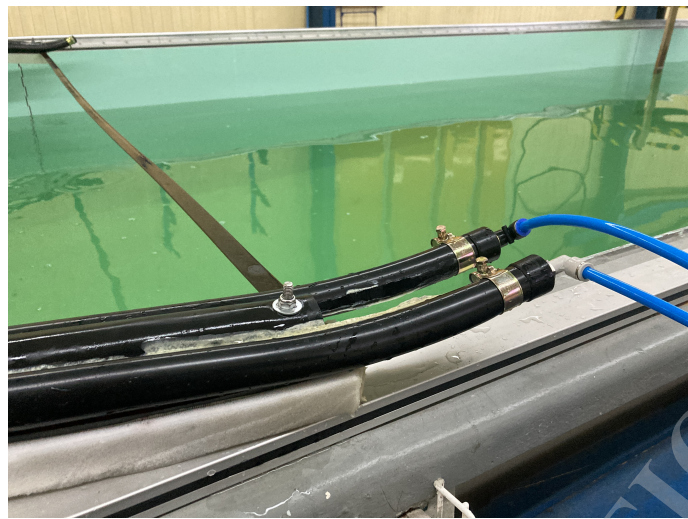


Figure 6: Configuration of the double-diffusor line.

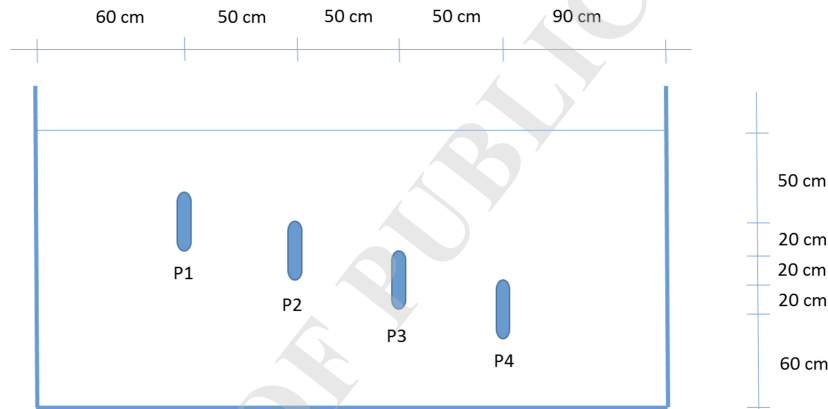


Figure 7: Hydrophone positions.

176 4.3 Curtains Configuration and Measurement Methodology.

177 The formula used to measure insertion loss IL is the one set by Equation 1, which is given by:

$$178 \quad 179 \quad 180 \quad 181 \quad 182 \quad 183 \quad IL = Lp_s - Lp_{x.x} \text{ dB}, \quad (1)$$

where

Lp_s : Sound pressure level generated by the loudspeaker at the position of the hydrophone and in the absence of the evaluated curtain, dB re.1 $[\mu\text{Pa}]$.

$Lp_{x.x}$: Sound pressure level generated by the loudspeaker at the position of the hydrophone and in the presence of the evaluated curtain, dB re.1 $[\mu\text{Pa}]$.

Table 3: Curtains configuration and measurement methodology.

Lp_{RF}	Background noise level present in the laboratory. Loudspeaker off.
Lp_{RFB}	Background noise level with Line 1, Line 2 and Line 3 working; each line with only one of their bubble curtains active. Loudspeaker off.
Lp_s	Level generated by the loudspeaker at the hydrophone position, without the presence of active curtains.
$Lp_{1.1}$	Level generated by the speaker at the hydrophone position, with Line 1 operating with only one of its bubble curtains active.
$Lp_{1.2}$	Level generated by the speaker at the hydrophone position, with Line 1 operating with both bubble curtains active.
$Lp_{3.1}$	Level generated by the speaker at the hydrophone position, with Line 3 operating with one of its bubble curtains active.
$Lp_{4.1}$	Level generated by the speaker at the hydrophone position, with Line 4 operating with one of its bubble curtains active.
$Lp_{1.1} + Lp_{2.1}$	Level generated by the speaker at the hydrophone position with Line 1 and Line 2 operating, with one of its bubble curtains active.
$Lp_{1.1} + Lp_{3.1}$	Level generated by the speaker at the hydrophone position with Line 1 and Line 3 operating, with one of its bubble curtains active
$Lp_{2.1} + Lp_{3.1}$	Level generated by the speaker at the hydrophone position with Line 2 and Line 3 operating, with one of its bubble curtains active
$Lp_{1.1} + Lp_{2.1} + Lp_{3.1}$	Level generated by the speaker at the hydrophone position, with Line 1, Line 2 and Line 3 operating, with one of its curtains active.
$Lp_{1.1} + Lp_{4.1}$	Level generated by the speaker at the hydrophone position with Line 1 and Line 4 operating, with one of its bubble curtains active.
$Lp_{1.1} + Lp_{3.1} + Lp_{4.1}$	Level generated by the speaker at the hydrophone position, with Line 1, Line 3 and Line 4 operating, with one of its curtains active.
$Lp_{1.1}, 25\%$	Level generated by the speaker at the hydrophone position, with Line 1 operating with the diffuser 1 at 25% of maximum airflow and the diffuser 2 at 0% of its maximum airflow.
$Lp_{1.1}, 50\%$	Level generated by the speaker at the hydrophone position, with Line 1 operating with the diffuser 1 at 50% of maximum airflow and the diffuser 2 at 0% of its maximum airflow.
$Lp_{1.1}, 75\%$	Level generated by the speaker at the hydrophone position, with Line 1 operating with the diffuser 1 at 75% of maximum airflow and the diffuser 2 at 0% of its maximum airflow.
$Lp_{1.1}, 100\%$	Level generated by the speaker at the hydrophone position, with Line 1 operating with the diffuser 1 at 100% of maximum airflow and the diffuser 2 at 0% of its maximum airflow.

Insertion loss IL is defined as the logarithmic ratio of the sound power transmitted by a system before the insertion of a noise control device to the sound power transmitted after insertion. This measure takes into account not only the performance of the noise control device, but also the effects of insertion, such as the alteration of the source's sound power or the generation of sound by the attenuator itself (Fahy, 2001).

In the subindex $x.x$ in Equation 1, the first x indicates the number of the line considered, which may be 1, 2, 3 or 4. The second x indicates the number of active diffusors per line, which may be 1 or 2. For example, $Lp_{1.1}$ corresponds to the noise level measured at the hydrophone

184

185

186

187

188

189

190

191

192 position, when Line 1 presents only one of its two bubble curtains working. $Lp_{1,2}$ refers to Line
 193 1 with its two bubble curtains operating. Figure 8a shows an example of Line 1 with only one
 194 of its diffusers or hoses active, and figure 8b, with both of its diffusers or hoses working.

195 The measurements were carried out in a laboratory environment, under controlled conditions,
 196 allowing comparative measurements of different air bubble curtain configurations.

197 Table 3 shows the different configurations of bubble curtains that were assessed during this
 198 study.

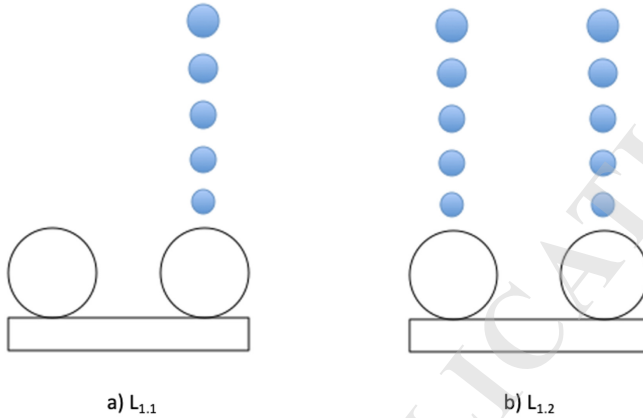


Figure 8: Example a. Line 1 with only one of its diffusers generating a bubble curtain. Example b. Line 1 with its two diffusers generating bubble curtains. .

199 5 Results

200 5.1 Measured Sound Pressure Levels

201 5.1.1 Background Noise Levels Lp_{BN} and Lp_{BNB}

202 Table 4 shows the sound pressure level Lp_{BN} recorded at the hydrophone location when the
 203 sound source is off and all bubble curtains are disconnected. It also provides the sound pressure
 204 level Lp_{BNB} , recorded under the same conditions except with all bubble curtains active. This
 205 allows for an evaluation of the noise produced by the bubble curtains themselves.

Table 4: Background noise levels measured at the four positions of the hydrophones with the
 loudspeaker off.

	Hydrophone position				Measured level dB re.1 μ Pa]
	P1	P2	P3	P4	
Lp_{BN}	117.9	117.6	118.3	118	118
Lp_{BNB}	119.8	119.9	120.4	120.2	120.1

206 5.1.2 Loudspeaker Level Lp_s Without Active Curtains

207 Table 5 shows the sound pressure level measured at the hydrophone position with the sound
 208 source operating and all bubble curtains deactivated.

Table 5: Sound pressure level measured at the hydrophone position with the loudspeaker driven by white noise and all bubble curtains disconnected.

	Hydrophone position				Measured level dB re.1[μ Pa]
	P1	P2	P3	P4	
Lp_s	160.8	161.1	163.3	161.2	161.7
Lp_s	160.9	161.6	163.5	161.4	161.9
Average value				161.8	

Figure 9 shows the frequency spectrum of the laboratory background noise, measured at the hydrophone position with no noise source present (Lp_{BN}). Similarly, it displays the frequency spectrum of the background noise with all bubble curtains active (Lp_{BNB}) and the frequency spectrum of the sound measured at the hydrophone position with the sound source driven by white noise, with no active curtain (Lp_s).

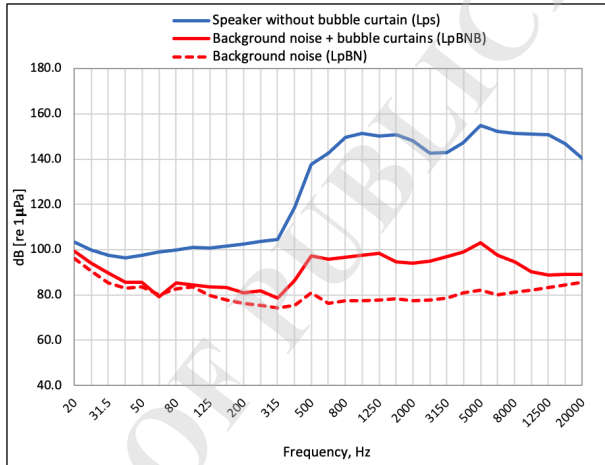


Figure 9: Third-octave band frequency spectra of the sound source and background noise of the laboratory and air generation system.

Although the speaker specifications state that its frequency response ranges from 200 Hz to 23 kHz, Figure 9 shows that below 200 Hz the speaker does emit sound and is capable of producing a sound pressure level at the hydrophone position higher than the background noise level. From 40 Hz upwards, the sound pressure level produced by the sound source at the hydrophone position is always higher than the background noise level, by 13 dB or more.

5.1.3 Levels Measured for Different Curtain Configurations

Table 6 shows the sound pressure levels at the hydrophone position during the different settings of the evaluated curtains, as shown in Table 3. We see that the sound pressure levels obtained by using the two bubble curtains or diffusers of Line 1 ($Lp_{1,2}$) are very similar to the levels obtained by using only one of the bubble curtains of Line 1 ($Lp_{1,1}$). This means that the line provides almost the same broadband attenuation in both cases. The data shows that reducing the air flow, from initially at a rate of 27 l/min, by half has virtually no effect on the achieved sound attenuation. Therefore, in all subsequent measurements, it was determined that only one of the two bubble curtains per line should be used.

Table 6: Sound pressure level measured at the hydrophone position with the loudspeaker driven by white noise and with different curtains configurations.

	Hydrophone position				Level dB re.1[μ Pa]
	P1	P2	P3	P4	
$Lp_{1.1}$	150.6	150.3	150.4	150.2	150.4
$Lp_{1.2}$	150.2	150	150.4	149.9	150.1
$Lp_{3.1}$	151.2	151	150.9	150.8	150.9
$Lp_{4.1}$	151.2	150.9	151	150.2	150.8
$Lp_{1.1} + Lp_{2.1}$	149.4	149.4	149.6	149.7	149.5
$Lp_{1.1} + Lp_{3.1}$	147.8	147.8	147.7	148.1	147.9
$Lp_{2.1} + Lp_{3.1}$	149.7	149.2	1479.2	149.5	149.4
$Lp_{1.1} + Lp_{2.1}$ + $Lp_{3.1}$	147.8	147.7	147.7	147.6	147.7
$Lp_{1.1} + Lp_{4.1}$	146.2	146.3	146.42	146.4	146.3
$Lp_{1.1} + Lp_{3.1}$ + $Lp_{4.1}$	145.6	145.3	145.8	145.5	145.6

228 Table 7 shows the levels obtained by modifying the percentage of the air flow of 27 l/min,
 229 applied to hose 1 of Line 1. Figures 10 to 15 present frequency band attenuation for each bubble
 230 curtain configuration listed in Table 6.

Table 7: Sound pressure level measured at the position P4 of the hydrophone, with the loudspeaker driven by white noise and modifying the air flow of diffuser 1 of Line 1.

Hydrophone position P4			
$Lp_{1.1}$ 25% dB re.1[μ Pa]	$Lp_{1.1}$ 50% dB re.1[μ Pa]	$Lp_{1.1}$ 75% dB re.1[μ Pa]	$Lp_{1.1}$ 100% dB re.1[μ Pa]
155.4	152.6	152	150.8

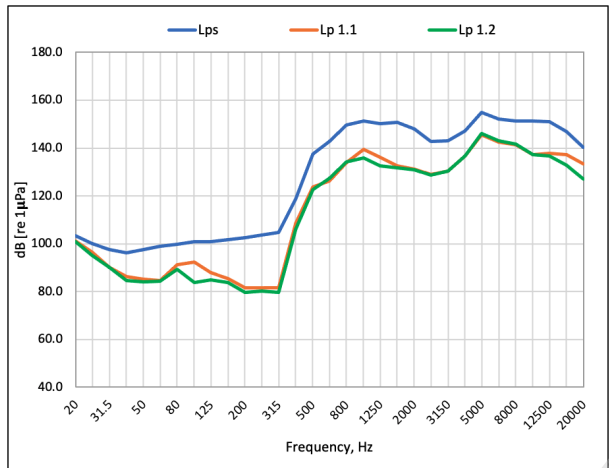


Figure 10: Third-octave band frequency spectra obtained for curtain configurations Lp_s , $Lp_{1.1}$ and $Lp_{1.2}$ (see Table 3).

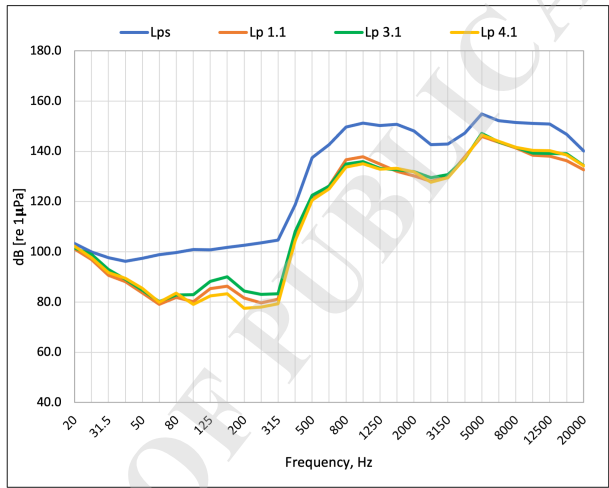


Figure 11: Third-octave band frequency spectra obtained for curtain configurations Lp_s , $Lp_{1.1}$, $Lp_{3.1}$ and $Lp_{4.1}$ (see Table 3).

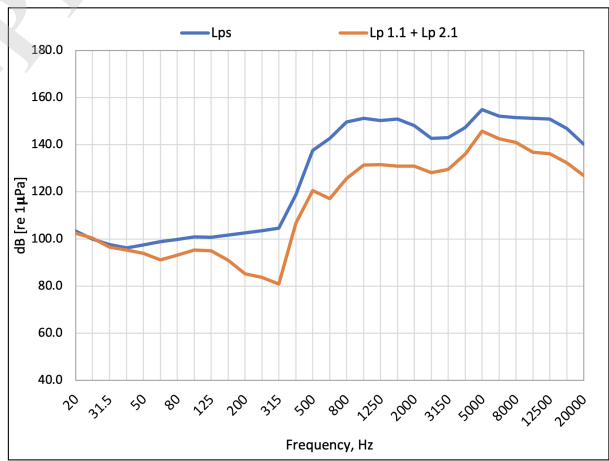


Figure 12: Third-octave band frequency spectra obtained for curtain configurations Lp_s and $(Lp_{1.1} + Lp_{2.1})$.

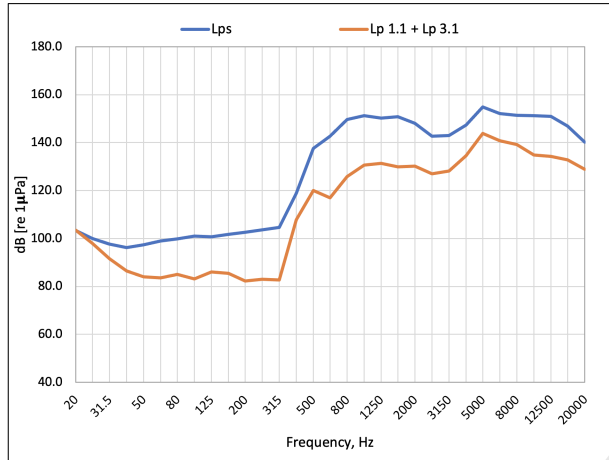


Figure 13: Third-octave band frequency spectra obtained for curtain configurations Lp_s and $(Lp_{1.1} + Lp_{3.1})$.

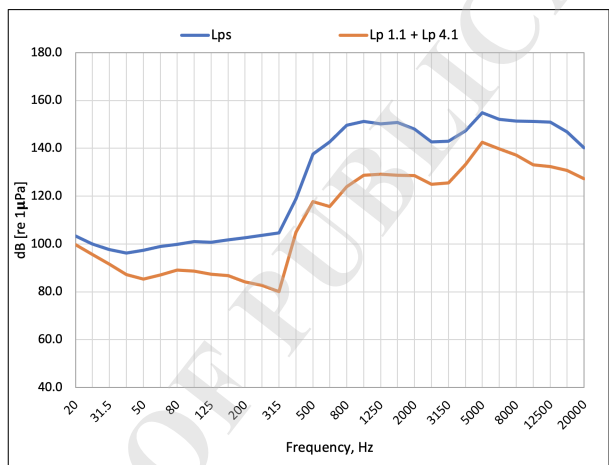


Figure 14: Third-octave band frequency spectra obtained for curtain configurations Lp_s and $(Lp_{1.1} + Lp_{4.1})$.

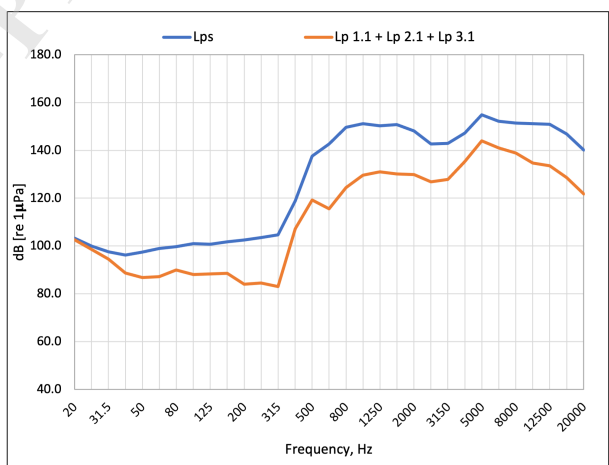


Figure 15: Third-octave band frequency spectra obtained for curtain configurations Lp_s and $(Lp_{1.1} + Lp_{2.1} + Lp_{3.1})$.

5.2 Insertion Loss IL

The insertion loss IL is estimated as the difference between the sound pressure level (Lp_s) measured without a curtain and the sound pressure level ($Lp_{x.x}$) measured when the curtain is active (Eq. 1). Table 8 shows the broadband IL values obtained for the different combinations of bubble curtains. The results demonstrate that using a single line does not affect the broadband insertion loss, regardless of the number of curtains per line ($Lp_{1.1}$ or $Lp_{1.2}$) or the distance of the line from the source or receiver. The various configurations of a single curtain result in an IL ranging from 11 to 12 dB. These attenuation values are consistent with some of the results obtained in field measurements (Nehls *et al.*, 2015). When using two lines, greater separation between the lines results in greater broadband insertion loss, with IL values increasing by up to 15.5 dB. The use of three lines causes only a slight further increase in insertion losses compared to two lines, reaching a level of 16.2 dB.

Table 8: Broadband Insertion Loss for the different configurations of bubble curtains evaluated. dB re.1[μ Pa]

Curtain configuration evaluated	Lp_s dB	$Lp_{x.x}$ dB	IL Broadband dB
$Lp_{1.1}$	161.8	150.4	11.4
$Lp_{1.2}$	161.8	150.1	11.7
$Lp_{3.1}$	161.8	150.9	10.9
$Lp_{4.1}$	161.8	150.8	11
$Lp_{1.1} + Lp_{2.1}$	161.8	149.5	12.3
$Lp_{1.1} + Lp_{3.1}$	161.8	147.9	13.9
$Lp_{1.1} + Lp_{4.1}$	161.8	146.3	15.5
$Lp_{1.1} + Lp_{2.1} + Lp_{3.1}$	161.8	147.7	14.1
$Lp_{1.1} + Lp_{3.1} + Lp_{4.1}$	161.8	145.6	16.2

It is imperative to establish the insertion loss for each frequency band. As illustrated in Figure 16, the insertion loss per third octave band for Line 1 is presented, considering both configurations: one active curtain $Lp_{1.1}$ and two active curtains $Lp_{1.2}$. As previously indicated in Tables 6 and 8, the IL per frequency band provided by Line 1 in both configurations is practically the same. The $Lp_{1.2}$ configuration is the most prevalent in salmon farming, where its attenuation is equal to or greater than 10 dB in virtually all frequency bands from 40 Hz upwards. This minimum attenuation is consistent with that reported in another study for similar curtains (Rustemeier *et al.*, 2012).

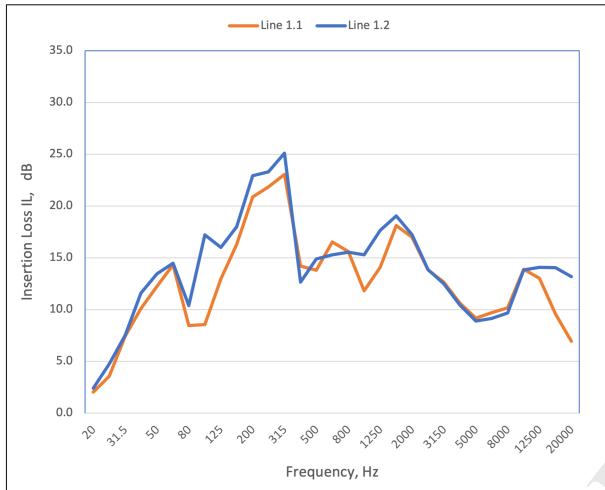


Figure 16: Insertion loss by frequency bands given by Line 1, configurations $Lp_{1.1}$ and $Lp_{1.2}$.

251 Figure 17 shows that, for the case of a single line, the position of the line between the source
 252 and the receiver will produce a change in the IL per frequency band. The closer the curtain
 253 is to the receiver, the greater the attenuation at low frequencies. This can be explained as an
 254 increase in the attenuation of low-frequency components mechanically transmitted through the
 255 bottom of the test channel.

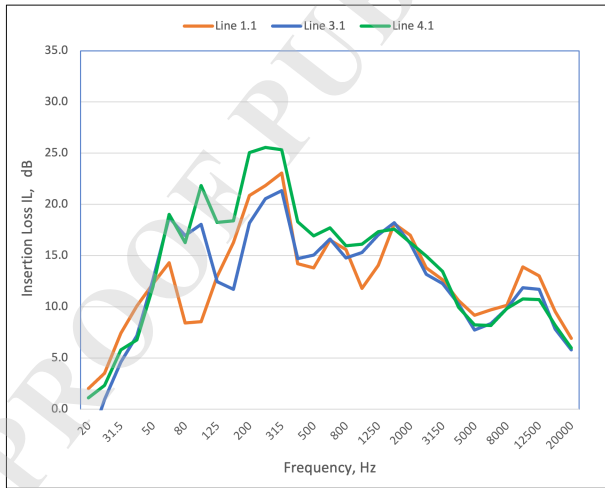


Figure 17: Insertion loss by frequency bands given by Line 1, configurations $Lp_{1.1}$, $Lp_{3.1}$ and $Lp_{4.1}$.

256 The employment of dual lines as opposed to a single line results in an increase in the IL
 257 per frequency band, with an increase from 400 Hz. The attenuation is directly proportional to
 258 the separation of the lines. As illustrated in Figure 18, utilising two lines instead of a single
 259 line results in a substantial enhancement of the IL , with the maximum occurring within the
 260 frequency range from 400 Hz to 2 kHz. This leads to IL values ranging from 15 to 27 dB.
 261 This frequency range corresponds with another study of bubble curtains (Beelen *et al.*, 2025).
 262 However, there, the IL values are considerably lower due to the limitations imposed by the low
 263 signal-to-noise ratio employed.

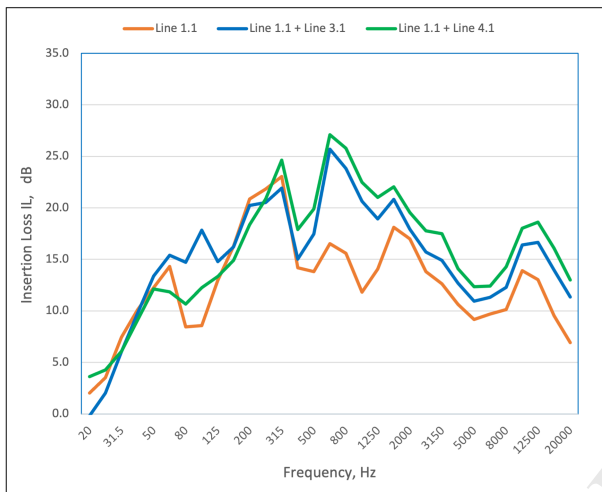


Figure 18: Insertion loss by frequency bands given by Line 1, configurations ($Lp_{1.1} + Lp_{3.1}$) and ($Lp_{1.1} + Lp_{4.1}$).

5.3 Air-bubble Curtains and Acoustic Impact Reduction

These days, bubble curtains are extensively employed as an underwater noise mitigation system; however, the extent to which the noise level of the sound source will be mitigated remains uncertain. The results of this study demonstrate that the evaluated bubble curtain will provide an *IL* attenuation greater than or equal to 10 dB in all frequency bands and all configurations. To comprehend the implications of a 10 dB reduction of a noise level, one must consider the acoustic impact area that would result from, for instance, pile driving operations, with and without the use of bubble curtains, as evaluated in this study. In order to assess the potential impact a project may have on marine species, it is first necessary to estimate the sound pressure level to which the species under study will be exposed. Equation 2 provides the noise level for each frequency band that a noise source generates at a given distance, considering the sound propagation model characteristic of the site.

$$Lr = SL - N \log(r) - \alpha \cdot r \text{ dB}, \quad (2)$$

with

Lr : Sound level per frequency band at a distance r , dB re.1[μPa].

SL : Source level per frequency band (Leq , Lp_{rms} , SEL), dB re.1[$\mu\text{Pa}\cdot\text{m}$] or dB re.1[$\mu\text{Pa}^2\cdot\text{s}\cdot\text{m}$]

N : Local attenuation ratio.

r : Distance from the source to the receiver, m.

α : Sound absorption per frequency band, dB/m.

In deep waters and in absence of sound channels, a spherical propagation is considered with $N = 20$. In presence of sound channels, a cylindrical propagation is considered with $N = 10$.

In shallow waters, sound propagation involves a large number of reflections of the acoustic signal at the surface and seabed, making it difficult to determine the N value that correctly describes the propagation (Jastrzebski, 2007; Khalilabadi, 2022; Lippert *et al.*, 2018). In the case of shallow waters, field measurements of attenuation at various distances from a noise source are typically conducted to obtain an empirical approximation of N , where values ranging from 13 to 35 are typically observed (Richardson *et al.*, 1995). As demonstrated in the relevant

292 literature, $N = 15$ has been shown to provide a high degree of fit with a significant number of
 293 measurements in shallow waters (MMO, 2015; NMFS, 2021; CALTRANS, 2020). Because of
 294 this, to describe sound propagation in our example a value $N = 15$ will be used.

295 Once the value of N has been selected or determined, the level Lr at different distances r
 296 from a source of known level SL can be predicted. Furthermore, the maximum distance at
 297 which the emitted sound can be perceived without generating negative effects in the receiver
 298 can be determined. To evaluate the physiological impact on the considered marine species, the
 299 sound levels per frequency band Lr obtained from Equation 2, or the source levels SL of the
 300 spectrum, must be weighted by the auditory weighting functions of each animal. Subsequently,
 301 a comparison of the results with the highest permitted thresholds according to the applied
 302 criterion is required. These thresholds are indicated in Table 2, corresponding to specific
 303 species of marine mammals.

304 Pile driving is a significant source of underwater noise, generating high levels of sound pres-
 305 sure. In the context of construction, this noise source is typically the primary focus during
 306 the initial phase of a project, as it is often the most distinct. Pile driving can easily reach
 307 broadband levels close to 200 dB re.1[μ Pa] at a distance of 1 m. Table 9 presents the levels
 308 emitted at a distance of 10 m during the driving of a steel pile with a diameter of 1.52 m. It
 309 should be noted that each strike lasted approximately 0.1 s on average.

Table 9: Sound pressure levels generated during the driving of 1.52 m diameter piles, mea-
 sured at a distance of 10 m and with a strike duration of 0.1 seconds (URS, 2011; Rodkin,
 Pommerenck, 2014)

Source	$L_{p_{peak}}$, dB re.1[μ Pa]	$L_{p_{rms}}$, dB re.1[μ Pa]	SEL , dB re.1[μ Pa 2 ·s]
Pile ϕ 1.52 m	210	195	185

310 By normalizing these values to the distance 1 m from the source, the source level SL can be
 311 obtained for the various noise descriptors, as demonstrated in Table 10.

Table 10: Estimated sound pressure levels at a distance of 1 m when driving a pile with a
 diameter of 1.52 m

. Calculated considering a sound propagation between spherical and cylindrical $15\log(r)$ (CAL-
 TRANS, 2020).

Source	$L_{p_{peak}}$, dB re.1[μ Pa]	$L_{p_{rms}}$, dB re.1[μ Pa·m]	SEL , dB re.1[μ Pa 2 ·s·m]
Pile ϕ 1.52 m	225	210	200

312 For instance, consider a pile driving rate of three piles per day, with an estimated 270 blows
 313 required for each pile. This results in a total of 810 blows, and the unweighted cumulative noise
 314 exposure level over a 24-hour period is $SEL_{cum24h} = 229.1$ dB.

315 Figure 19 presents the third-band used for our noise source, based on data from 1.6 m diameter
 316 pile driving (Nehls *et al.*, 2007). The amplitude was adjusted so its broadband level matches
 317 the cumulative sound exposure level in our example.

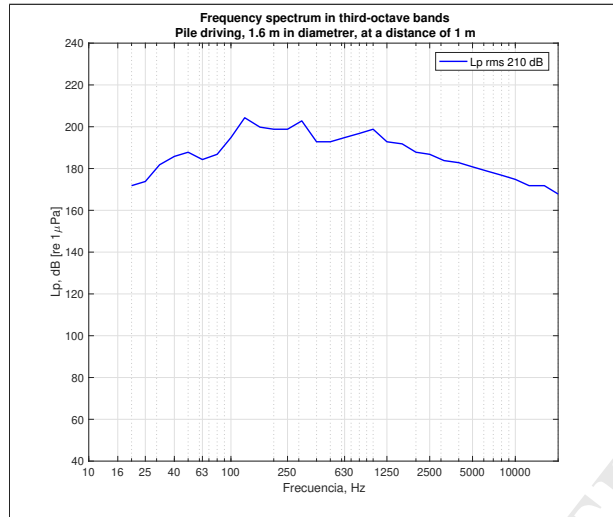


Figure 19: Third-octave band frequency spectrum obtained for driving 1.6 m diameter piles (Nehls *et al.*, 2007).

Table 11 summarizes the distances at which the TTS and AUD INJ thresholds are reached for five groups of marine mammals due to pile driving of 1.52 m, according to the NMFS 2024 criteria (NOAA, 2024) with auditory weighting for the five animal groups. Figures 20 and 21 show the distance dependence of the weighted SEL for LF and HF mammals, respectively, and the threshold distances assuming an attenuation ratio of $15\log(r)$.
 318
 319
 320
 321
 322

Table 11: Evaluation of physiological effects as a result of driving 1.52 m diameter piles without the use of air bubble curtains. Auditory injury INJ and temporal threshold shift TTS according to NMFS 2024 criterion (NOAA, 2024). Estimated considering sound propagation as $15\log(r)$ (CALTRANS, 2020). dB re. $1[\mu\text{Pa}^2 \cdot \text{s}]$.

Group	SEL_{cum24h} , dB Weighted	Threshold TTS dB	Distance TTS, m	Threshold AUD INJ dB	Distance AUD INJ, m
LF	227.2	168	5490	183	821
HF	214.7	178	273	193	28
VHF	201.3	144	3497	159	588
OW	212.4	170	630	185	67
PW	219.6	168	2231	183	268

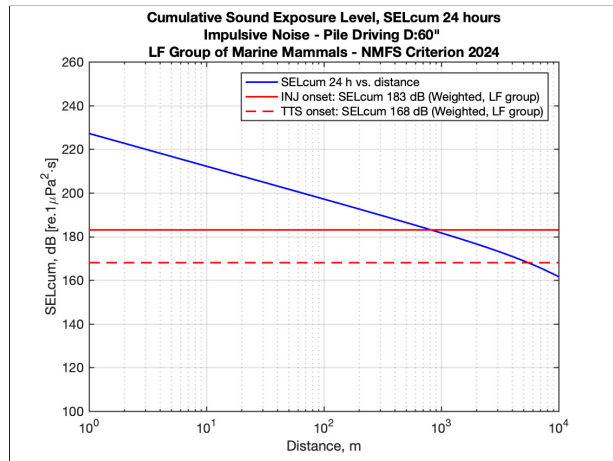


Figure 20: Physiological impact ranges of sound emissions during pile driving on low-frequency (LF) marine mammals. Attenuation factor $15\log(r)$.

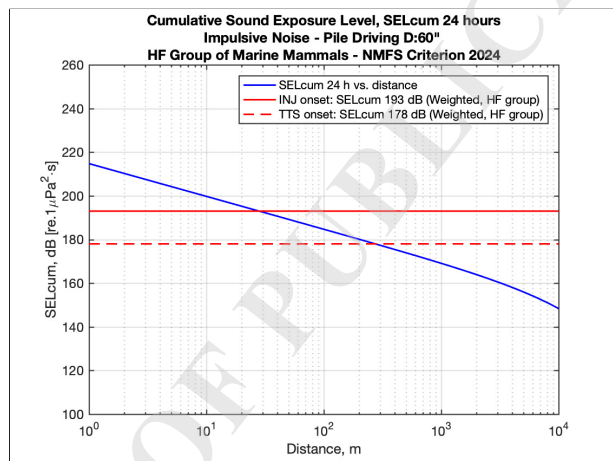


Figure 21: Physiological impact ranges of sound emissions during pile driving on high-frequency (HF) marine mammals. Attenuation factor $15\log(r)$.

323 Using a bubble curtain as tested here can reduce pile driving noise by at least 10 dB per
 324 frequency band, even in its basic form $Lp_{1.2}$. Using a conservative criterion, the spectrum levels
 325 in Figure 19 can be reduced by 10 dB, thus reducing the SEL_{cum24h} level from 229.1 dB to 219.1
 326 dB. Table 12 and Figure 22 illustrate how such attenuation decreases distances of occurrence
 327 of exceeding TTS and AUD INJ thresholds for high-frequency cetaceans.

Table 12: Assessment of physiological effects on the species considered as a result of driving 1.52 m diameter piles and using air bubble curtains as a mitigation measure. Estimated considering a sound propagation between spherical and cylindrical $15\log(r)$ (CALTRANS, 2020). dB re.1 $[\mu\text{Pa}^2 \cdot \text{s}]$

Group	SEL_{cum24h} , dB Weighted	Threshold TTS dB	Distance TTS, m	Threshold AUD INJ dB	Distance AUD INJ, m
LF	217.2	168	1183	183	177
HF	204.7	178	59	193	6
VHF	191.3	144	753	159	126
OW	202.4	170	136	185	14
PW	209.6	168	481	183	58

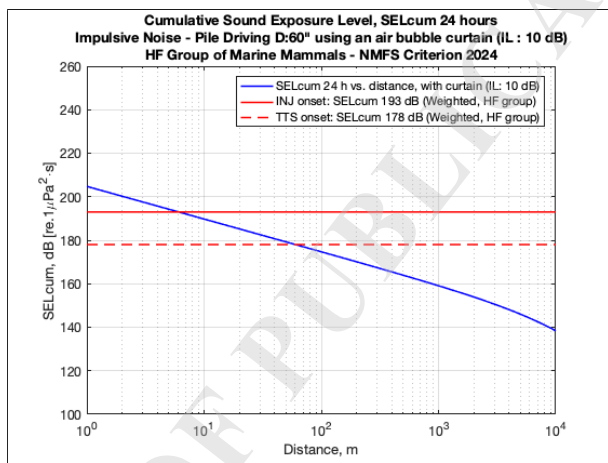


Figure 22: Evaluation of the physiological effects on high frequency cetaceans HF due to pile driving and the use of an air bubble curtain (IL: 10 dB).

By comparing Tables 11 and 12, it is clear that with a conservative approach, employing an air bubble curtain that provides at least 10 dB of attenuation in each frequency band leads to at least a 78.4% reduction in the distances at which the TTS and AUD INJ thresholds are reached. This equates to a substantial decrease in the effects of pile driving on the region's native marine fauna.

6 Discussion

The measurements were conducted under favorable background noise conditions, yielding a signal-to-noise ratio of at least 13 dB for frequencies above 40 Hz. The background noise level reached 120.1 dB with the bubble generation system active and 118 dB with the system inactive, both referenced to 1 micropascal. Sound levels produced by the loudspeaker were measured at four distinct hydrophone positions to reduce potential wave cancellation within the test channel, thereby enhancing the signal-to-background noise ratio. On average, the loudspeaker generated a broadband level of 161.8 dB at the measurement points, resulting in a signal-to-noise ratio of 41.7 dB.

328
329
330
331
332
333
334
335
336
337
338
339
340
341

342 With respect to attenuation achieved by a single line, in the case of Line 1—whether employing
 343 a single active bubble curtain $Lp_{1.1}$ or two active bubble curtains $Lp_{1.2}$ —delivers a broadband
 344 insertion loss IL between 11 dB and 12 dB (Table 8). This suggests that the line can maintain
 345 its sound attenuation performance using only one hose. The dual curtain setup $Lp_{1.2}$ yields
 346 higher IL at some frequencies but does not notably improve broadband IL overall (Figure 16).

347 Considering individual lines attenuation, Lines 1, 3, and 4 exhibit similar broadband insertion
 348 loss IL , each presenting values in the region of 11 dB (Table 8). This observation indicates
 349 that the specific distance of a line from either the noise source or the receiver does not signif-
 350 icantly influence the broadband IL . Despite the broadband similarities, notable differences in
 351 the insertion loss are observed in third-octave frequency bands (Figure 17). Specifically, the at-
 352 tenuation at low frequencies increases in the case of lines positioned closer to the receiver. This
 353 phenomenon can be attributed to the mechanical transmission of noise through the bottom of
 354 the test channel, followed by its re-radiation into the water. It is important to note that if this
 355 transmission pathway through the channel floor were eliminated, the frequency-dependent IL
 356 data would likely converge and become more uniform across the different line positions.

357 When evaluating the use of two lines, the broadband IL varies between 12.3 dB for con-
 358 figuration $Lp_{1.1} + Lp_{2.1}$ and 15.5 dB for configuration $Lp_{1.1} + Lp_{4.1}$. This suggests that a
 359 greater separation between the lines results in a higher insertion loss. Addition of a third line
 360 between two active lines leads to a modest increase in total insertion loss, with an enhancement
 361 of less than 1 dB. In these cases, the maximum insertion loss reaches 16.2 dB (Table 8 for
 362 configurations $Lp_{1.1} + Lp_{2.1} + Lp_{3.1}$ and $Lp_{1.1} + Lp_{3.1} + Lp_{4.1}$).

363 For third-octave band insertion loss, single lines offer an IL between 10 dB and 25 dB, ensuring
 364 that single lines always achieve at least 10 dB of broadband attenuation. Enhancing the signal-
 365 to-noise ratio at frequencies below 40 Hz could further raise this minimum attenuation. In
 366 contrast, double lines provide an IL from 11 dB to 27 dB and cover a broader frequency range
 367 than single lines. Their highest attenuation is between 400 Hz and 2 kHz.

368 Comparing Tables 11 and 12 reveals that using a bubble curtain achieving 10 dB IL in each
 369 frequency band reduces the distance at which physiological damage thresholds are reached by
 370 78.4%.

371 For the LF cetacean group—which includes species like blue, humpback, and fin whales—Table
 372 11 indicates that any individual within 821 meters of pile driving activity risks auditory injury
 373 (AUD INJ) during a 24-hour exposure. With air bubble curtains providing 10 dB noise atten-
 374 uation, this risk zone is reduced from 821 m to 177 m (refer to Table 12). For threshold shift
 375 (TTS) in the LF group, the affected distance decreases from 5490 m to 1183 m.

376 In the HF group individuals within distance below 3497 m of pile driving risk TTS, and those
 377 within 588 m risk AUD INJ; employing bubble curtains reduces these distances to 753 m and
 378 126 m, respectively (see Tables 11 and 12).

379 7 Conclusion

380 The results of this study demonstrate that the bubble curtains evaluated function effectively
 381 as acoustic barriers and can serve as a viable underwater noise mitigation measure, aligning
 382 with the new requirements of the Chilean Environmental Assessment Service for controlling
 383 high energy anthropogenic underwater noise.

384 Laboratory measurements of insertion loss IL enabled systematic comparison of different
 385 bubble curtain configurations under stable and controlled conditions, thereby avoiding the
 386 variability inherent in field measurements.

Across all tested configurations, the air bubble curtains achieved an *IL* of at least 10 dB in every frequency band. Applying a conservative criterion, the evaluated bubble curtain—when deployed as a mitigation measure for pile driving—would provide a minimum attenuation of 10 dB per frequency band, even in its simplest configuration. This reduction translates into a decrease of at least 78.4% in the physiological risk area for marine mammals.

It should be noted, however, that attenuation performance in the field may vary depending on factors such as signal-to-noise ratio (SNR), seabed sound transmission, and the variation of the structural integrity of the bubble curtain with depth and ocean currents.

References

Servicio de Evaluación Ambiental (2022), *Criterio de Evaluación en el Sistema de Evaluación de Impacto Ambiental SEIA: Predicción y Evaluación de Impactos por Ruido Submarino*, SEA.

Rustemeier J., Griebmann T., Rolfes R. (2012), Underwater sound mitigation of bubble curtains with different bubble size distributions, *Proceedings of Meetings on Acoustics*, Vol. **17**.

Division of Environmental Analysis California Department of Transportation. (2020), *Technical Guidance for the Assessment of Hydroacoustic Effects of Pile Driving on Fish*, Caltrans.

Würsig B., Greene C.R., Jefferson T.A. (2000), Development of an air bubble curtain to reduce underwater noise of percussive piling. *Marine Environmental Research*, **49**(1), 79–93.

Dähne M., Tougaard J., Carstensen J., Rose A., Nabe-Nielsen J. (2017), Bubble curtains attenuate noise from offshore wind farm construction and reduce temporary habitat loss for harbour porpoises, *Mar Ecol Prog Ser*, Vol. **580**, 221–237.

Lucke K., Blanchet M.A., Siebert U. (2011), The use of an air bubble curtain to reduce the received sound levels for harbor porpoises (*Phocoena phocoena*), *J Acoust Soc Am*, **130**, 3406–3412.

Novarini J.C., Keiffer R.S., Norton G.V. (1998), A model for variations in the range and depth dependence of the sound speed and attenuation induced by bubble clouds under wind-driven sea surfaces, *IEEE Journal of Oceanic Engineering*, **23**, 423–438.

Hall M.V. (1989), A comprehensive model of wind generated bubbles in the ocean and predictions of the effects on sound propagation at frequencies up to 40 kHz, *The Journal of the Acoustical Society of America*, **86**, 1103–1117.

Göttsche K.M., Juhl P.M., Steinhagen U. (2013), Numerical prediction of underwater noise reduction during offshore pile driving by a small bubble curtain, *Proceedings Internoise: Noise Control for Quality of Life*.

Chao Qi, Zuxiang Hu, Suihong Wang, Zhixiong Jiang, Haoyuan Wu, Zhiqiang Yin (2021), Study on the Propagation Law of Water Hammer Wave in Underwater Blasting and the Reducing Effect of Air Curtain on Water Hammer Wave, *Shock and Vibration*, Article ID 9994071, doi.org/10.1155/2021/9994071.

Tsouvalas A. (2020), Underwater Noise Emission Due to Offshore Pile Installation: A Review, *Energies*, **13**, 3037; doi:10.3390/en13123037.

426 Strietman W.J., Michels R., Leemans E., (2018), *Measures to reduce underwater noise and*
 427 *beach litter, An assessment of potential additional measures for the Netherlands*, Wageningen
 428 Economic Research, Report 2018-087.

429 Koschinski S., Ludemann K., (2013), *Development of Noise Mitigation Measures in Offshore*
 430 *Wind Farm Construction*, Federal Agency for Nature Conservation.

431 OSPAR (2014), *Inventory of Measures to Mitigate the Emission and Environmental Impact of*
 432 *Underwater Noise-Technical Report*, OSPAR Commission.

433 Bellmann M.A., (2014), Overview of existing noise mitigation systems for reducing pile-
 434 driving noise, *INTER-NOISE and NOISE-CON Congress and Conference Proceedings*, **249**,
 435 2544–2554.

436 JNCC (2010). Joint Nature Conservation Committee, *Statutory Nature Conservation Agency*
 437 *Protocol for Minimising the Risk Injury to Marine Mammals from Piling Noise*. Aberdeen,
 438 UK.

439 Werner S. (2010), *Towards a Precautionary Approach for Regulation of Noise Introduction*
 440 *in the Marine Environment from Pile Driving*, Federal Environmental Agency, Stralsund.
 441 Germany.

442 Lucke K., Siemersma M. (2013), *International regulations on the impact of pile driving noise*
 443 *on marine mammals – A literature review*, Institute for Marine Resources and Ecosystem
 444 Studies.

445 Fahy F. (2001), *Foundations of Engineering Acoustics*, Elsevier academic press, ISBN 0-12-
 446 247665-4

447 Richardson W.J., Greene C.R., Malme C.I., Thomson D.H. (1995), *Marine mammals and noise*,
 448 Academic Press Inc., New York.

449 Urick R.J. (2010), *Principle of underwater sound*, Peninsula Publishing, Third edition.

450 Robinson S.P., Lepper P.A., Hazelwood R.A. (2014), *Good Practice Guide for Underwater Noise*
 451 *Measurement*, National Measurement Office, Marine Scotland, The Crown Estate, NPL Good
 452 Practice Guide No. 133, ISSN: 1368-6550, 2014.

453 Möser M., Barros J.L. (2004), *Ingeniería Acústica, Teoría y Aplicaciones*, ISBN 3-00-014278-9.
 454 2004.

455 Medwin H. (2005), *Sounds in the Sea, From Ocean Acoustics to Acoustical Oceanography*,
 456 Cambridge University Press.

457 National Marine Fisheries Service (2018), *Revisions to: Technical Guidance for Assessing the*
 458 *Effects of Anthropogenic Sound on Marine Mammal Hearing (Version 2.0): Underwater*
 459 *Thresholds for Onset of Permanent and Temporary Threshold Shifts*, U.S. Dept. of Commer.,
 460 NOAA. NOAA Technical Memorandum NMFS-OPR-59.

461 National Marine Fisheries Service (2024), *Update to: Technical Guidance for Assessing the*
 462 *Effects of Anthropogenic Sound on Marine Mammal Hearing (Version 3.0): Underwater and*
 463 *In-Air Criteria for Onset of Auditory Injury and Temporary Threshold Shifts*. U.S. Dept. of
 464 Commer., NOAA. NOAA Technical Memorandum NMFS-OPR-71, 182 p.

Departament of Arts, Heritage and the Gaeltacht (2014), *Guidance to manage the risk to marine mammals from man-made sound sources in Irish waters.* 465
466

Department of Planning, Transportation and Infrastructure (DPTI) (2012), *Underwater Piling Noise Guide*, Government of South Australia. 467
468

McKenzie C. (2015), *Smalandsfarvandet Offshore Wind Farm Underwater Noise*, Energinet.dk. 469

Yori A. (2018), Underwater Assessment of Anthropogenic Noise Sources Using a Field Recording Method, *Acta Acustica United with Acustica*, **104**, 13 – 24. 470
471

Southall et al. (2019), Marine Mammal Noise Exposure Criteria: Updated Scientific Recommendations for Residual Hearing Effects, *Aquatic Mammals*, **45**(2), 125-232. DOI 472
473
474

Southall et al. (2007), Marine Mammal Noise Exposure Criteria: Initial Scientific Recommendations, *Aquatic Mammals*, Vol. **33**, 4. 475
476

MMO (2015), *Modelled mapping of continuous underwater noise generated by activities, A report produced for the Marine Management Organization*, MMO Project No: 1097, ISBN: 477
478
479

National Marine Fisheries Service (2021), *Guidelines for Non-lethally Deterring Marine Mammals*, <https://jmlondon.shinyapps.io/NMFSAcousticDeterrentWebTool/> 480
481

Jastrzebski, S. (2007), Application of Time Reversal Technique in Shallow Water Environment, *Archives of Acoustics*. Vol. **32**, No. 4, 319–324. 482
483

Khalilabadi, M. (2022), 2D Modeling of Wave Propagation in Shallow Water by the Method of Characteristics. *Archives of Acoustics*. Vol. **47**, No. 3, pp. 407–412, doi: 484
485
486

URS (2011), *Report Marine Noise Assessment*, Northern Territory Department of Lands and Planning. Australia. 487
488

Rodkin R., Pommerenck K. (2014), Caltrans compendium of underwater sound data from pile driving. *Inter Noise 2014*. 489
490

Nedwell J. R., Edwards B., Turnpenny A.W.H. (2004), *Fish and Marine Mammal Audiograms: A summary of available information*, Subacoustech Report ref: 534R0214. 491
492

Nehls, G., Betke, K., Eckelmann, S., Ros. M. (2007), *Assessment and costs of potential engineering solutions for the mitigation of the impacts of underwater noise arising from the construction of offshore windfarms*, BioConsult SH report, Husum, Germany. On behalf of COWRIE Ltd. 493
494
495
496

Nehls, G., Rose, A., Diederichs, A., Bellmann, M., Pehlke, H. (2015), *Noise Mitigation During Pile Driving Efficiently Reduces Disturbance of Marine Mammals*, *Advances in Experimental Medicine and Biology*, **875**, 755–762. 497
498
499

Parvin S. J., Nedwell J. R. (1995), Underwater Sound Perception and the Development of an Underwater Noise Weighting Scale, *Underwater Thechnology*, Volumen **21**, number 1. 500
501

502 Beelen S., Nijhof M., de Jong C., van Wijngaarden L., Krug D. (2025), Bubble curtains for noise
503 mitigation: One vs two, *The Journal of the Acoustical Society of America*, **157**, 1336–1355.

504 Lippert T., Ainslie M., von Estorff O. (2018), Pile driving acoustics made simple: Damped
505 cylindrical spreading model, *The Journal of the Acoustical Society of America*, **173**, 310–317.

506 Nedwell J. R., Turnpenny A.W.H., Lovell J., Parvin S.J., Workman R., Spinks J.A.L., Howell
507 D. (2007), A validation of the dBht as a measure of the behavioural and auditory effects of
508 underwater noise. Subacoustech Report No. 534R1231.

PRE-PROOF PUBLICATION ARCHIVES OF ACOUSTICS